

Received March 25, 2021, accepted March 28, 2021, date of publication March 31, 2021, date of current version April 9, 2021.

Digital Object Identifier 10.1109/ACCESS.2021.3070066

# MSD-Based NMPC Aircraft Anti-Skid Brake Control Method Considering Runway Variation

MENGQIAO CHEN<sup>1</sup>, FENGRUI XU<sup>1</sup>, XUELIN LIANG<sup>1</sup>, AND WENSHENG LIU<sup>1,2</sup>

<sup>1</sup>School of Automation, Central South University, Changsha 410083, China

<sup>2</sup>Advanced Research Center, Central South University, Changsha 410083, China

Corresponding author: Wensheng Liu (liuwensheng@csu.edu.cn)

This work was supported in part by the Chang Jiang Scholars Program of Ministry of Education of China under Grant T2011119.

**ABSTRACT** In this paper, a nonlinear model predictive control (NMPC) method based on mixed slip-deceleration (MSD) with runway identification is proposed to prevent the aircraft wheels from locking up and improve the braking performance under time-varied runway conditions. The MSD control algorithm reduces the dependence of control performance on slip rate estimation accuracy and retains a good slip rate control performance. The proposed NMPC control method guarantees optimal braking torque on each wheel by individually controlling the slip rate of each wheel near the optimal point. A nonlinear brake control model based on aircraft ground taxiing dynamics is derived. In this model, the tire-runway friction coefficient–slip rate model under different runway conditions and vertical force variation caused by brake are considered. A runway identification algorithm based on friction coefficient and friction coefficient slope is used to identify the real-time runway status, based on which the prediction model and optimization function of the proposed control scheme are modified. The wheel slip stable zone and the system maximum brake torque are regarded as time-domain constraints of the NMPC for safety considerations and physical limitations. The control objectives of the NMPC include longitudinal deceleration, braking performance, and preservation of crew comfort. The proposed MSD-based NMPC controller is verified by a tricycle-gear aircraft model using MATLAB/Simulink software. Simulation results of different control schemes on a specific mixed runway show good performances of the proposed control method. The proposed control method provides a new efficient solution for aircraft wheel braking on variable runway.

**INDEX TERMS** NMPC, mixed slip-deceleration control, aircraft brake control, runway identification.

## I. INTRODUCTION

The brake control of aircraft has always been an important research subject since it has a great influence on the safety of aircraft ground operation. While taxiing on a runway, an aircraft utilizes air resistance, reverse engine thrust, and other methods to decelerate. However, the most effective and reliable way to decelerate is to brake by wheels. The main function of the anti-skid brake control system is to decelerate the aircraft according to the pilots' braking instructions and avoid unsafe incidents during the braking process, which includes tire burst and runway veer off.

The aircraft body and wheel rotation dynamic characteristics of the braking process are complex due to the highly nonlinear and uncertain tire-runway friction characteristics, which makes the realization of anti-skid braking control

for achieving high efficiency and safety a challenging task. In addition, with the development of the aviation industry, other requirements for the brake control system design, such as economy and comfort, have gradually become indispensable. Therefore, the problems of nonlinearity and uncertainty, runway state estimation and adaptability problem, and multi-objective optimization are the key issues of aircraft anti-skid braking control.

To solve the problems of nonlinearity and uncertainty, feedback-based control methods have been proposed, including PID control [1]–[3], feedback linearization, sliding mode control [4], and intelligent control [5]. In [1], a nonlinear control based on the error feedback using the Lyapunov function was presented, and the experimental results showed that the proposed methods could accomplish the braking process in less time and shorter distance compared with the PID controller based on the linearized system. A sliding mode controller based on a piecewise linear model was proposed

The associate editor coordinating the review of this manuscript and approving it for publication was Haibin Sun<sup>1</sup>.

in [4], and simulation results showed that the proposed controller had a good control effect on runway friction coefficient changing and might excite unmodeled dynamics. In [6], an adaptive sliding mode controller based on the feedback linearization with a sliding observer was proposed; it could estimate the unmeasurable vehicle velocity and solve the problem of time-delayed input by treating it as a bounded uncertainty. A nonlinear output feedback controller based on bounded brake torque was proposed in [7]. By using the combination of set point on-line adaption based on slip rate and the brake torque, the proposed controller could significantly enhance the brake performance in a double  $\mu$ -jump braking maneuver. A model-free Q-learning approach to nonlinear state-feedback ABS slip control was proposed in [5] to address the unmodeled dynamics and parametric uncertainty caused by high nonlinearity. Although this approach does not require an initial stabilizing controller, a large number of transition samples are needed for learning when advanced features, such as setpoint tracking, are required at various speeds. In [8], a robust sliding mode controller was proposed. This controller compares two nonlinear observers to estimate vehicle velocity. The results have shown that the sliding observer is promising while the extended Kalman filter is unsatisfactory due to unpredictable changes in the road conditions.

From the aspect of runway environmental adaptability, the uncertainty of runway state has a great influence on braking control performance, and an adaptive algorithm based on tire-runway state estimation is an effective brake control method. In recent years, research on dynamic state estimation in the field of vehicle dynamics control has developed significantly [9], and the state estimation of the tire-runway characteristics of the aircraft brake control has become similar to that of a vehicle. In [10], an algorithm based on the Kalman filter supported by a change detection algorithm was proposed to estimate the slip slope; however, it was designed to work under normal driving conditions, so it is inactive under the conditions of sharp bends, braking, torque changes, and skidding. The sign of slip slope was used to supervise the system state through estimation with or without wheel slip measurements [11]. In [12], a nonlinear observer was proposed for tire-road adhesion coefficient and linear vehicle velocity using only the measurement of rotational wheel velocity, and a lumped friction model was used to approximate the distribute friction model for simplification. In [13], a method of slip slope estimation from wheel velocity based on the on-line least-squares method was presented, and the estimation performance was experimentally verified.

In the field of multi-objective brake control, most of the anti-skid brake control methods have been focusing on tracking the best deceleration performance, that is, tracking the optimal skid rates or maximum deceleration rate of an aircraft [1], [2]. However, in addition to the deceleration performance, other factors, such as comfort and economy, should also be considered. Multi-objective optimization algorithms have been applied to anti-skid control [14]–[16] to

improve the comprehensive performance of brake control. Model predictive control (MPC) is a rolling optimization control method based on a prediction model. The MPC has a good control performance in anti-skid brake control, which represents a multi-objective optimization problem with constraints, and it also has good robustness against external disturbance and model uncertainty.

The brake control system operates under certain constraints [14], [17], [18], including the physical constraint of the brake control valve, safety constraint of the wheel slip rate, and safety constraint of the output brake torques. In addition, the slip rate feedback control is based on the slip rate estimation. The slip rate estimation error is caused by the measurement noise of the wheel speed as well as the measurement or estimation error of aircraft speed depending on how the aircraft speed is obtained. In this work, feedback errors are regarded as wheel speed measurement noise and slip rate estimation error since the wheel speed and the aircraft velocity can be regarded as the measurement signals for the controller.

Based on the above thorough analysis, the existing multi-objective optimization control methods of anti-skid braking are merely feedback control methods based on the slip rate estimation and do not consider the influence of runway condition variation. Therefore, a multi-objective anti-skid braking control method that can handle runway changes and measurement noise is urgently needed. This paper presents a mixed slip-deceleration-based nonlinear model predictive control (NMPC) aircraft anti-skid brake control method. The mixed slip-deceleration (MSD) control method can suppress the influence of noise and reduce the dependence on the accuracy of slip rate estimation [19]–[21]. The main advantages of the MSD-NMPC are as follows. The model predictive control can handle complex optimization problems and constraints [22], [23]. It can also manage multiple control requirements while considering the weighting matrix and can incorporate all control objectives in one formulation. In addition, the control parameters can be easily tuned. Further, the time-domain constraints, such as valve maximum limitations and performance metrics, are considered. Furthermore, it has a certain decoupling ability for a coupling control system. Besides, it is not sensitive to slip rate estimation error. Different runway conditions are identified by the designed identification algorithm, and the prediction model and evaluation function are switched according to the identification results so as to achieve optimal performance on different runways. The control method can effectively prevent the wheel from slipping while constraining the output pressure and slip rate within a safe range. An improved MSD control method is also used for comparison. The simulation case studies and analytical discussions are presented to demonstrate the effectiveness and adaptability of the proposed control method.

The rest of the paper is organized as follows. Section 2 analyzes the characteristics and control problems of the aircraft anti-skid brake control system. Section 3 introduces the MSD-based NMPC control scheme designed for the anti-skid brake control system. Section 4 presents the simulation

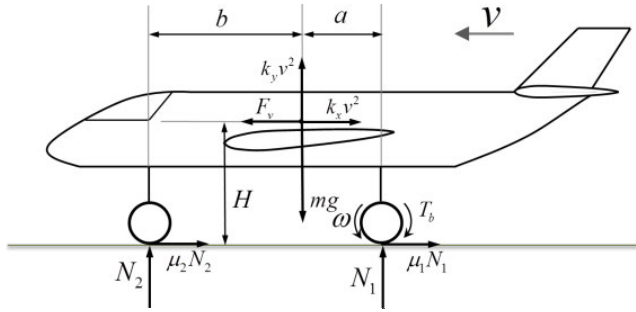


FIGURE 1. Dynamical model of aircraft during braking process.

results and discussion. Finally, Section 5 concludes the paper and presents future work directions.

## II. CONTROL-ORIENTED SYSTEM MODEL AND PROBLEM STATEMENT

In order to design an MSD control scheme for the aircraft brake control system, a nonlinear brake control system model based on aircraft ground taxiing dynamics is developed. The nonlinearity of the brake control system mainly comes from its dynamic characteristics and nonlinearity of the tire-runway model. The brakes of wheels are controlled independently, but there is a certain degree of coupling between wheels. The larger the number of brake wheels is, the lower the degree of coupling will be. The safety issue is a comprehensive problem in which longitudinal and lateral dynamics should be jointly considered. However, this paper mainly focuses on the influence of the control system on the aircraft's longitudinal dynamic performance. To deal with the control problem easily, certain assumptions and neglects are made to study the aircraft dynamics in the longitudinal direction; namely, lateral, pitch, and roll dynamics are not considered, and no additional effects as active dampers/springs or stabilizers are modeled.

### A. DYNAMIC MODEL OF BRAKE CONTROL SYSTEM

This paper selects a tricycle-gear aircraft as a research object. The dynamic performances of the aircraft body and wheels are studied as shown in Fig. 1, considering only the longitudinal movement and pitching motion that affects wheel loads while neglecting lateral, vertical, yawing, and rolling movements. The dynamic equations of the aircraft body movement and wheel rotation are as follows:

$$\begin{cases} J\dot{\omega}_i = r\mu_i N_i - T_{bi} \\ m\dot{v} = -\sum_i \mu_i N_i - \mu_{front} N_{front} + F_v - k_x v^2 \\ \sum_i N_i + N_{front} = mg - k_y v^2 \\ \sum_i \mu_i N_i H + \sum_i N_i a + \mu_{front} N_{front} H - N_{front} b = 0 \end{cases} \quad (1)$$

where  $\omega$  denotes the wheel angular speed and  $v$  represents the longitudinal speed of the aircraft body;  $N_1$  and  $N_{front}$  are the vertical loads at the contact points of the main wheels and

nose wheels, respectively;  $\mu_1$  and  $\mu_2$  are the tire-road friction coefficients of the main wheel and nose wheel, respectively;  $T_b$  is the braking torque on the braking discs;  $F_v$  denotes the engine residual thrust;  $k_x$  and  $k_y$  are the air resistance coefficients in the horizontal and vertical directions, respectively;  $H$  represents the height of the center of aircraft gravity;  $a$  and  $b$  are the horizontal distances from the center of aircraft gravity to the main wheels and nose wheels, respectively; lastly,  $J$ ,  $r$ ,  $m$ , and  $g$  are the momentum of inertia of the main wheel, the main wheel radius, the aircraft mass, and the gravitational acceleration, respectively.

### B. LONGITUDINAL SLIP AND DECELERATION CALCULATION MODE

The longitudinal slip rates and deceleration rates of the brake wheels denote the input of the MSD control algorithm. The slip rate is an important factor affecting the tire-road adhesion and system stability. The deceleration rate used in this paper is defined as a normalized linear wheel deceleration, and wheel slip is defined as follow:

$$\begin{cases} \eta_i = -\frac{\dot{\omega}_i r}{g} \\ \lambda_i = \frac{v - \omega_i r}{v} \end{cases} \quad (2)$$

### C. TIRE-RUNWAY FRICTION COEFFICIENT MODEL

The tire-runway friction coefficient  $\mu_i$  depends on a large number of parameters, including the parameters of road, tire, speed, load, and the depth of slip. A simple empirical "magic formula" model developed by Pacejka has been widely used, and it is expressed as [24]:

$$\mu(\lambda; \theta_j) = \theta_1 \sin(\theta_2 \cdot \arctg(\theta_3 \cdot \lambda)) \quad (3)$$

where  $\theta_j$  is defined by tire conditions, road conditions, and aircraft velocity. In this paper, three magic formulas of typical runways are used: dry runway, wet runway, and ice runway, which represent the ranges of high, medium, and low adhesion coefficient tire-runway conditions, respectively. Subsequent runway settings and identification algorithm are based on these three types of tire-runway models, which are as follows:

$$\text{Dry runway: } \mu(\lambda) = 0.8 \cdot \sin(1.5344 \cdot \arctg(14.0326\lambda))$$

$$\text{Wet runway: } \mu(\lambda) = 0.4 \cdot \sin(2.0192 \cdot \arctg(8.2098\lambda))$$

$$\text{Ice runway: } \mu(\lambda) = 0.2 \cdot \sin(2.0875 \cdot \arctg(7.201788\lambda))$$

### D. CONTROL ORIENTED MODEL

To design a control law, a nonlinear model based on aircraft dynamics is developed. By substituting the expression  $\dot{\lambda} = -\frac{r}{v}\dot{\omega} + \frac{r\omega}{v^2}\dot{v}$  derived from (2) into (1), the following equation is obtained:

$$\begin{aligned} \dot{\lambda}_i = & - \left[ \frac{r^2}{vJ} \mu_i(\lambda_i) N_i + \frac{(1-\lambda_i)}{mv} \sum_i \mu_i(\lambda_i) N_i \right. \\ & \left. + \frac{(1-\lambda_i)}{mv} \mu_{front} N_{front} \right] \end{aligned}$$

$$+ \frac{rT_{bi}}{vJ} + \frac{(1 - \lambda_i)F_v}{mv} - \frac{v(1 - \lambda_i)k_x}{m} \quad (4)$$

Then, by replacing  $\eta = -\frac{\dot{r}}{g}$  into (1), the expression of the wheel deceleration rate is obtained as:

$$\eta_i = -\frac{r}{gJ} (r\mu_i(\lambda_i)N_i - T_{bi}) \quad (5)$$

With the objective of controlling the skid depth or the deceleration of wheel, the dynamic relations between the system input instruction  $T_b$  and the output  $\lambda$  or  $\eta$  are studied. Equations (4) and (5) can be expressed as follows:

$$\begin{cases} \dot{\lambda} = \phi(\lambda) + \gamma T_b \\ \eta = \varphi(\lambda) + \xi T_b \end{cases} \quad (6)$$

According to the dynamic balance equations of an aircraft, which are given in the last two equations of (1),  $N_i$  can be analytically described as follows:

$$\begin{cases} N_i = \frac{1}{4} \frac{b - \mu_{front}H}{a + b + (\sum_i \mu_i - \mu_{front})H} (mg - k_y v^2) \\ N_{front} = \frac{a + \sum_i \mu_i H}{a + b + (\sum_i \mu_i - \mu_{front})H} (mg - k_y v^2) \end{cases} \quad (7)$$

**E. PROBLEM STATEMENT**

The function of the anti-skid brake control system is to decelerate the aircraft under maximum or designed deceleration capability while ensuring aircraft safety. This paper does not study the control strategy of the brake system under asymmetric conditions but considers the brake control in the longitudinal direction of the aircraft ground motion with no yaw trend, i.e., the yaw moment caused by a difference in the brake pressure on the left and right gears, which can be caused by the servo valve difference, brake disc coefficient difference or fluctuation, and other factors. This yawing moment can be compensated by the lateral force of the front wheel of an aircraft without using the differential control of the main wheels.

An important development direction of the modern aircraft brake control system is to ensure safety and meet various requirements simultaneously, which is different from the traditional brake control with only anti-skid protection. In the design of the anti-skid brake control system, the following control requirements should be considered:

- 1) The wheels should not be locked during the braking process under any conditions;
- 2) Different braking performance requirements should be satisfied depending on the use cases, such as maximum braking efficiency, specified deceleration rate, specified braking distance, comfort, and economy;
- 3) Constraints need to be considered in the controller design process.

First, in order to ensure the safety of aircraft operation, wheel locking is absolutely not allowed to happen because a short time of locking can result in severe tire wear and a rapid increase in the temperature, thus causing tire air leak or even

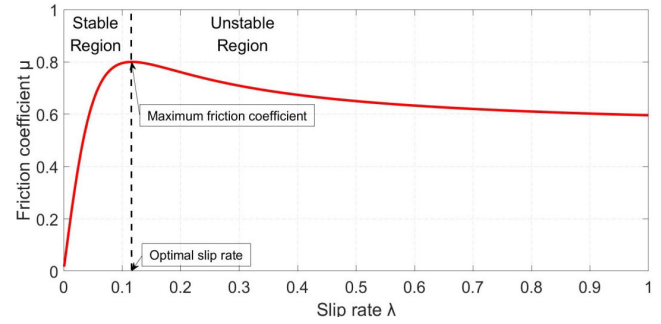


**FIGURE 2.** Relationship between the longitudinal slip rate and tire-runway adhesion coefficient.

burst. Previous studies have derived the direct relationship between the longitudinal slip rate and tire-runway adhesion coefficient, as shown in Fig 2. As shown in Fig. 2, there is a maximum value of the adhesion coefficient, and the corresponding slip rate is called the optimal slip rate. When the slip rate is less than the optimal slip rate, a region is defined as a stable region because the equilibrium points in this region are all stable. When the slip rate is greater than the optimal slip rate, the wheel tends to be completely locked without extra control. Since the equilibrium points are unstable, this region is called the unstable region. The anti-skid control should keep the slip rates out of the unstable region to avoid a deep slip or wheel locking. It is not a physical constraint, and it is mainly determined by the control strategy, so it can be considered as a soft constraint of a system.

It should be noted that the optimal slip rate is different for different runway conditions. In this paper, the optimal slip rates of dry, wet, and ice runways are studied, and the online identification method is used to capture the optimal slip rate under different working conditions so as to realize the automatic adjustment of the optimization function and the slip rate constraints.

In addition, the physical limitations of the actuator outputs should also be considered in the design of constraints. Since the hydraulic supply of the aircraft brake system is limited, the brake torque outputs of the system can be regarded as rigidly constrained, which can be expressed as follows:

$$0 \leq T_b \leq T_{b \max}$$

From the perspective of safety, the torque output limit of a system is judged by the severity of the wheel skid. Therefore, in the high-speed phase of the aircraft taxiing, the maximum value of the braking torque is relatively small because the loads on wheels are small due to the aerodynamic lift. With a decrease in the aircraft taxiing speed and an increase in the wheel loads, the maximum safety brake torque increases. The brake torque constraint is a time-varying constraint. However, it is difficult to define the function of this constraint because the wheel loads can be neither measured nor precisely predicted. The brake torque constraint is assigned to a constant value. With the slip rate constraint and output torque



constraint, operation safety can be guaranteed, and braking performance can be improved.

In addition to high braking efficiency, the comfort of pilots and passengers is also an optimization goal. Therefore, the goal is to minimize the variation in the output torque to achieve a smooth brake, especially in the field of civil aviation. In addition, the life of brake discs, energy consumption, and other economic indicators should be included in the optimization goal as long as needed.

According to the above discussion, the aircraft brake control problem can be described as a constrained multi-objective optimization control problem, thus:

- Multiple control objects should be considered
- Aiming at ensuring aircraft safety and preventing a wheel from locking up, the longitudinal slip  $\lambda$  must be limited within the stable zone.
- Furthermore, due to the brake maximum output torque limitation, control input  $T_b$  has to satisfy the hard constraint.
- In order to achieve good longitudinal acceleration and braking performance under various runway conditions, an appropriate large longitudinal force should be provided to each wheel.
- A trade-off between the aircraft safety and braking performance improvement should be achieved in the presence of additional objectives as well as aircraft safety constraints.

The nonlinearity of the tire-runway characteristic, multiple objectives, and the above-mentioned constraints make the control problem challenging. The NMPC is well known for its capability of dealing with complex optimization control problems as well as handling nonlinearities and constraints, and the MSD can reduce the dependence of the algorithm on the accuracy of the slip rate calculation. Therefore, this paper combines the NMPC method with MSD to solve the control problem.

### III. MSD-BASED NMPC CONTROLLER DESIGN

In this section, an MSD-based NMPC controller is designed to solve the constrained optimization control problem. The proposed control scheme is shown in Fig. 3. The MSD-based NMPC controller is the main controller that generates four brake torque outputs based on the information from the slip rate/deceleration rate calculation and runway identification. The wheel slip rates and deceleration rates are estimated based on the measured wheel angular speed and estimated aircraft velocity, which are used to construct a new compound control variable—the mixed slip-deceleration variable. The control feedback loop is based on mixed variables to reduce the dependence of the algorithm on the accuracy of the slip rate calculation. According to the estimated values of tire-runway adhesion force and vertical wheel load, the adhesion coefficient and slope of runway identification are calculated to estimate the runway state. The runway identification algorithm can identify the runway state in real-time. The main controller deals with the problem of the runway state switching by modifying the prediction model of the NMPC, which improves system adaptability to runway variation.

The NMPC algorithm uses a prediction model to predict future dynamics of the controlled object and operates by solving the optimization problem to determine the input sequence that satisfies the optimization function and constraints over a specified control time domain at each time step using the knowledge about the current system state variables and previous system inputs. Furthermore, after finding an optimal input sequence, the first input sequence is applied to the control system, and this process of prediction and optimization is repeated while the anti-skid braking function is active. The aircraft safety objective and actuator physical restriction are achieved by introducing the wheel slip stable zone constraints and output torque constraints, and the control objectives are realized by summing different optimization functions.

It should be noted that accurate values of related variables, such as aircraft speed, wheel angular speed, slip rate, and friction coefficient, are usually measured or estimated. The measurement noise and estimation error can lead to the deviation of a variable from its actual value, thus degrading the control performance. The proposed MSD control algorithm can reduce the dependence of the control performance on the slip rate estimation accuracy and maintain good slip rate control performance. As for the other variables, this paper does not consider the impact of their estimation accuracies and assumes that they can meet the performance requirements.

#### A. DISCRETE PREDICTION MODEL

According to the aircraft brake control model presented in Section II, the state space expression of the brake control can be expressed as follows:

$$\begin{cases} \dot{\lambda}_i = - \left[ \frac{r^2}{vJ} \mu_i(\lambda_i) N_i + \frac{(1-\lambda_i)}{mv} \sum_i \mu_i(\lambda_i) N_i \right. \\ \quad \left. + \frac{(1-\lambda_i)}{mv} \mu_{front} N_{front} \right] \\ \quad + \frac{(1-\lambda_i) F_v}{mv} - \frac{v(1-\lambda_i) k_x}{m} + \frac{r}{vJ} u_i \\ \eta_i = - \frac{r}{gJ} (r \mu_i(\lambda_i) N_i - u_i) \\ y_i = \varepsilon_i = \alpha \lambda_i + (1-\alpha) \eta_i \end{cases} \quad (8)$$

where  $i = lo, li, ri, ro$ ,  $x = [\lambda_{lo}, \lambda_{li}, \lambda_{ri}, \lambda_{ro}, \eta_{lo}, \eta_{li}, \eta_{ri}, \eta_{ro}]^T$  is the state variable,  $u = [T_{blo}, T_{bli}, T_{bri}, T_{bro}]^T$  is the control input, and  $y = [\varepsilon_{lo}, \varepsilon_{li}, \varepsilon_{ri}, \varepsilon_{ro}]^T$  is the system output that represents a linear combination of the slip rate and deceleration rate with the weighting coefficient  $\alpha$ .

In order to define a finite dimensional optimal control problem, the Euler method is used to discretize the system state-space model. The sampling period is denoted as  $\Delta t$ , and it is set according to the system nonlinear characteristics. The estimation error will be large if  $\Delta t$  is too large, which can lead to the infeasible solution to the optimization problem. The prediction period will be shorter if  $\Delta t$  is too small, which can increase the calculation amount of the optimization algorithm. The discrete system can be expressed as follows: (9) and (10), as shown at the bottom of the next page, where

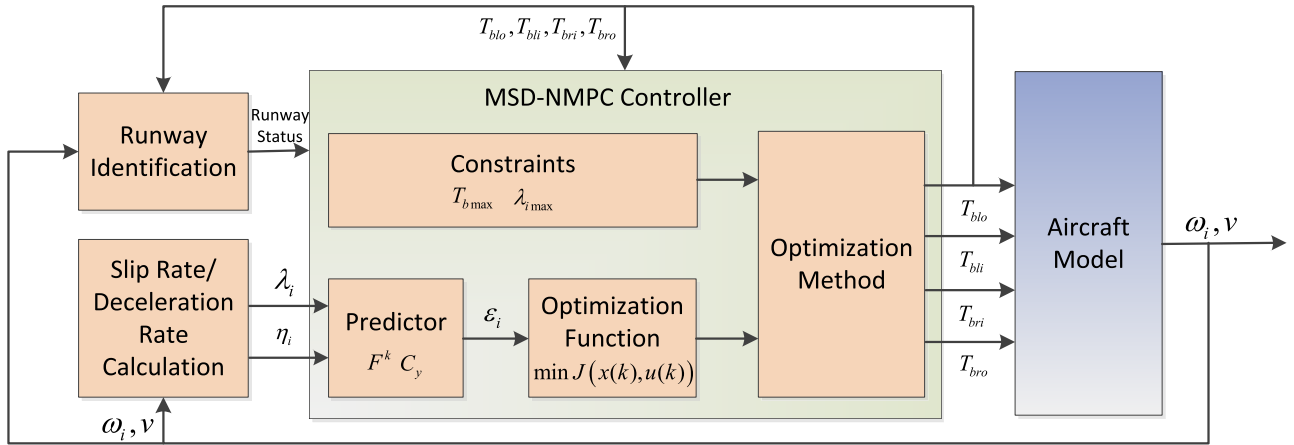


FIGURE 3. The structure of the proposed MSD-based NMPC controller.

$F^k$  represents the forward computing function of the system at time  $k$ , and  $C_y$  denotes the output matrix.

Assume  $N_p$  and  $N_c$  denote the predictive and control horizons, respectively, and  $N_p \geq N_c \geq 1$ . At the sampling time  $k$ , the control sequence  $U(k)$  (the optimization vectors) and system output sequence  $Y(k)$  are expressed as follows:

$$U(k) = \begin{bmatrix} u(k|k) \\ u(k+1|k) \\ \vdots \\ u(k+N_c-1|k) \end{bmatrix},$$

$$Y(k) = \begin{bmatrix} y(k+1|k) \\ y(k+2|k) \\ \vdots \\ y(k+N_p|k) \end{bmatrix}, \quad R(k) = \begin{bmatrix} r(k+1) \\ r(k+2) \\ \vdots \\ r(k+N_p) \end{bmatrix}$$

where  $R(k)$  denotes the reference matrix of the output variables, and  $r(k)$  is the optimal value of the mixed slip rate and deceleration rate at time  $k$ , which can be expressed as:

$$r(k) = [\varepsilon_{lo}(k), \varepsilon_{li}(k), \varepsilon_{ri}(k), \varepsilon_{ro}(k)]^T.$$

Therefore, the prediction process of the system state variables and system outputs at time  $k$  is defined as:

$$\begin{cases} x(k+i|k) = F^k(x(k+i-1|k), u(k+i-1|k)), \\ \quad 1 \leq i \leq N_c \\ y(k+i|k) = C_y(F^k(x(k+i-1|k), u(k+i-1|k))), \\ \quad 1 \leq i \leq N_p \end{cases} \quad (11)$$

Thus, to predict the system state and output at the next moment, it is needed to know the system state  $x(k|k)$  at the current moment. The optimal output sequences of the system at the current moment are obtained by the NMPC optimal algorithm, and the optimal control variable  $u(k|k)$  at the current moment is applied to the NMPC output. At each moment, a new optimization problem is solved.

### B. RUNWAY IDENTIFICATION ALGORITHM

Based on the above analysis, the tire-runway friction coefficient is directly related to the slip rate, and the friction coefficient model greatly affects the characteristics of the system model. Therefore, in order to make a prediction model be closer to the actual system under the time-varying conditions, the runway identification algorithm needs to be used.

The tire-runway friction coefficient model has been introduced in Section II. Additionally, as mentioned previously,

$$\left\{ \begin{aligned} \lambda_i(k+1) = & \left\{ \begin{aligned} & -\left[ \frac{r^2}{vJ} \mu_i(\lambda_i(k)) N_i + \frac{(1-\lambda_i(k))}{mv} \sum \mu_i(\lambda_i(k)) N_i \right] \\ & + \frac{(1-\lambda_i(k))}{mv} \mu_{front} N_{front} + \frac{(1-\lambda_i(k)) F_v}{mv} \\ & - \frac{v(1-\lambda_i(k)) k_x}{m} + \frac{r}{vJ} u_i(k) \end{aligned} \right\} \cdot \Delta t + \lambda_i(k) \end{aligned} \right. \quad (9)$$

$$\left\{ \begin{aligned} \eta_i(k+1) = & -\frac{r}{gJ} (r \mu_i(\lambda_i(k+1)) N_i - u_i(k+1)) \\ y_i(k) = & \varepsilon_i(k) = \alpha \lambda_i(k) + (1-\alpha) \eta_i(k) \end{aligned} \right. \Rightarrow \begin{cases} x(k+1) = F^k(x(k), u(k)) \\ y(k) = C_y x(k) \end{cases} \quad (10)$$

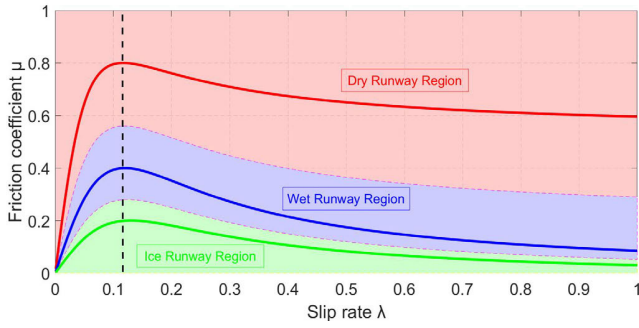


FIGURE 4. 2D region division of the friction coefficient–slip rate curves on different runways.

this paper studies three typical types of runways: dry runway, wet runway, and ice runway.

As shown in Fig. 4, the relationship between the friction coefficient and slip rate is different under different runway conditions. At the same slip rate, the dry runway has the maximum friction coefficient, while the ice runway has the minimum friction coefficient among all runway types. Therefore, the runway state can be identified by a two-dimensional region division of the friction coefficient and slip rate curves, as shown in Fig. 4. The input signal of the identification algorithm consists of the slip rate and friction coefficient. The slip rate can be calculated from the wheel speed signal and the aircraft ground speed signal, while the friction coefficient needs to be estimated by the inverse dynamic model of the wheel rotation, which has the braking torque and the wheel angular acceleration as inputs.

The friction coefficient is estimated as follows:

$$\mu = \frac{F_f}{F_N} = \frac{(T_b - \dot{\omega}J)/r}{f(\lambda, V)} \quad (12)$$

In the region of a low slip rate of the friction coefficient–slip rate curve, the friction coefficients of different runways are close to each other. Therefore, in this paper, another method is used for identification. In the stable region of the friction coefficient–slip rate curve, which is the region on the left side of the maximum friction coefficient, the slopes of the three curves are clearly different and independent of the slip rate. Based on this characteristic, a two-dimensional curve of the friction coefficient and the slope of friction coefficient in the stable region is obtained, as shown in Fig. 5. The three runway states can be identified by a two-dimensional region division of the curve. The input signals are the friction coefficient and the friction coefficient slope. The friction coefficient slope is calculated by dividing the friction coefficient change value by the slip rate change value as follows:

$$\kappa_k = \frac{\mu_k - \mu_{k-1}}{\lambda_k - \lambda_{k-1}} \quad (13)$$

The runway state is identified in real-time by a combination of the two above-presented methods, and a worse identified runway state is taken as a final identification result of the logical operation. It should be noted that the runway identification

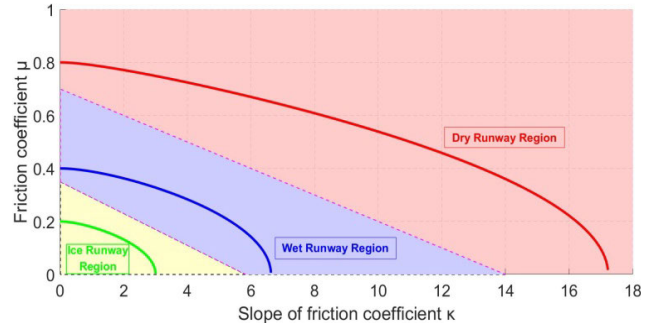


FIGURE 5. 2D region division of the friction coefficient–friction coefficient slope curves in the stable region.

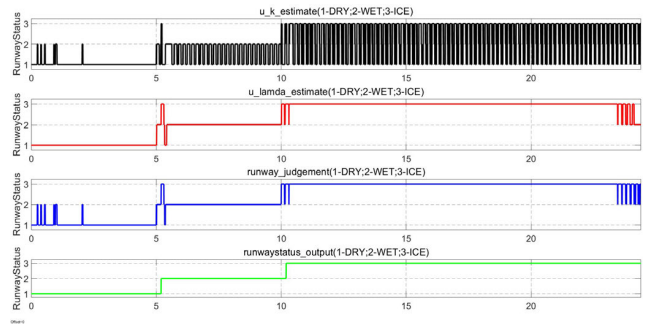


FIGURE 6. Performance of the identification algorithm on a mixed runway having the following structure: 0–5 s dry runway, 5–10 s wet runway, and after 10 s ice runway.

algorithm solves the problem of non-optimal control parameters and poor control performance caused by the runway state change, rather than improving the instantaneous control performance. Therefore, the identification period, namely the model switching interval, can be longer than the control period. In this study, the time window is denoted as  $T$ , and the runway state is identified from  $(k - 1)T$  to  $kT$  at time  $kT$ . The mean filtering method is used to process the identification input signals in a single time window. The runway state at time  $kT$  is determined by the values of the current variables in the two-dimensional region. The performance of the identification algorithm on a mixed runway is shown in Fig. 6, where it can be seen that the identification result has a time lag of  $T$  when the runway state is switched, which is acceptable from the aspect of the final control effect of the system.

### C. OPTIMIIZATION FUNCTION DESIGN

According to the characteristics of the constrained optimization problem described in Section II, it is necessary to solve the optimization problem at each step to obtain the best control effect. The optimization variables are the four brake torques output by the system. Based on different optimization objectives, the optimization function at time  $k$  consists of three parts, which are as follows.

1) The main purpose of the control algorithm is to obtain the minimum system tracking error, that is, to make the actual control output quickly tracked to the expected control output.

The future control output  $y(k+j|k)$  at time  $k$  can be obtained by the discrete prediction model presented in Section 3.1, and the expected control output  $r(k+j)$  is set in advance according to the runway identification results. The first part of the optimization function is designed as follows:

$$J_1 = \sum_{j=1}^{N_p} \|y(k+j|k) - r(k+j)\|_S^2 = \sum_{j=1}^{N_p} \sum_i \left[ S_i (\varepsilon_i(k+j|k) - r_i(k+j))^2 \right] \quad (14)$$

where  $S$  denotes the weighting matrix used to adjust the weight of the tracking error of each wheel.

2) Considering crew comfort, the brake torque output should change as slowly as possible to ensure the braking process is smooth. The second part of the optimization function consists of the sum of changes in the control variable, which can be expressed as follows:

$$J_2 = \sum_{j=0}^{N_c-1} \|\Delta u(k+j|k)\|_P^2 = \sum_{j=0}^{N_c-1} \sum_i \left[ P_i \Delta T_{bi}(k+j|k)^2 \right] \quad (15)$$

where  $\Delta u$  denotes the change rate of the system output with a weighting matrix  $P$ .

3) In order to avoid the infeasible problem, the relaxation variable is added to the slip rate variable and used to form a penalty term of the optimization function so that the slip rate falls in the stable region as far as possible, which can be expressed as:

$$J_3 = \sum_i \|s_{i(opt)}\|_{\kappa}^2 \quad (16)$$

where  $s_{(opt)}$  denotes the relaxation variable on the constraints of the slip rate used to avoid the infeasible problem, and  $\kappa$  is a weighting matrix.

The optimization function of the NMPC consists of the three parts given above, while the constraints are designed according to the description in Section II as follows:

$$J(x(k), u(k)) = J_1 + J_2 + J_3 = \sum_{j=1}^{N_p} \|y(k+j|k) - r(k+j)\|_S^2 + \sum_{j=0}^{N_c-1} \|\Delta u(k+j|k)\|_P^2 + \sum_i \|s_{i(opt)}\|_{\kappa}^2$$

$$s.t. \quad 0 \leq T_{bi}(k+j|k) \leq T_{b\max}, \quad j = 0, 1, \dots, N_c - 1,$$

$$-s_{i(opt)} \leq \lambda_i(k+j|k) \leq \lambda_{i\max} + s_{i(opt)},$$

$$s_{i(opt)} \geq 0, \quad j = 1, \dots, N_p \quad (17)$$

The dynamic constraints of the above-described optimization problem are derived from the physical constraint of the

maximum brake torque and the soft constraint of the slip rate safety range.

#### D. CONTROL OUTPUTS AND ONLINE OPTIMIZATION

To obtain the minimum value of the optimization function  $J(x(k), u(k))$  under the constraint conditions, the optimization algorithm can be used to calculate an optimal output sequence at the current moment. The model predictive control adopts a rolling finite time domain optimization strategy; namely, the optimization process is not completed at once offline but repeatedly performed online.

The optimization strategy of the NMPC can be seen as a nonlinear programming problem. In this study, the optimization routine E04WD of the NAG toolbox is used to solve the optimization problem. The E04WD is designed to minimize an arbitrary smooth function subject to constraints that can include simple bounds on variables, linear constraints, and smooth nonlinear constraints by using a sequential quadratic programming (SQP) method [25], which is effective in solving this type of nonlinear programming problem of the NMPC. According to the NMPC control strategy, the first element of  $U(k)$  is implemented as a control output of the NMPC controller as follows:

$$u(k) = [1, 0, \dots, 0] \cdot U(k) \quad (18)$$

where  $u(k)$  denotes a set of optimal vectors of brake torques and works as a control signal to the brake control system. The described procedure is repeated at each sampling interval.

### IV. SIMULATIONS AND ANALYSIS

The proposed MSD-based NMPC controller was verified by simulations in the MATLAB/Simulink environment. According to the engineering structure of a tricycle-gear aircraft with dual wheels, a full-vehicle model was built in MATLAB/Simulink, as shown in Fig. 7. The built model mainly includes the aircraft body, wheel, and controller models.

#### A. PARAMETERS SETTING

The simulation sample step and the sampling period of the prediction model were 0.005 s. The weighting factors and the prediction and control horizons were set as follows:  $S_i = 1$ ,  $P_i = 2e - 7$ ,  $\kappa_i = 1$ , ( $i = lo, li, ri, ro$ );  $N_p = 3$ ,  $N_c = 3$ ,  $T_{b\max} = 138000Nm$ ,  $\lambda_{i\max} = 0.13$ .

The prediction and control horizons were chosen based on the tradeoff between the computing capacity and prediction accuracy. The upper bound of the brake torque was the system's maximum capability, and the upper bound of slip rate was the maximum value of the stable boundary of different runway conditions.

The weight factor  $S_i$  was a positive weighting factor used to adjust the tracking performance; it played a regulatory role in maintaining stable control and better control performance;  $P_i$  was a positive weighting factor used to coordinate the rate of change of the control output  $T_b$ , and enlarging  $P_i$  could make the control output change smoothly;  $\kappa_i$  was a positive penalty factor of slack variables  $s_{i(opt)}$ , and enlarging  $\kappa_i$  could make



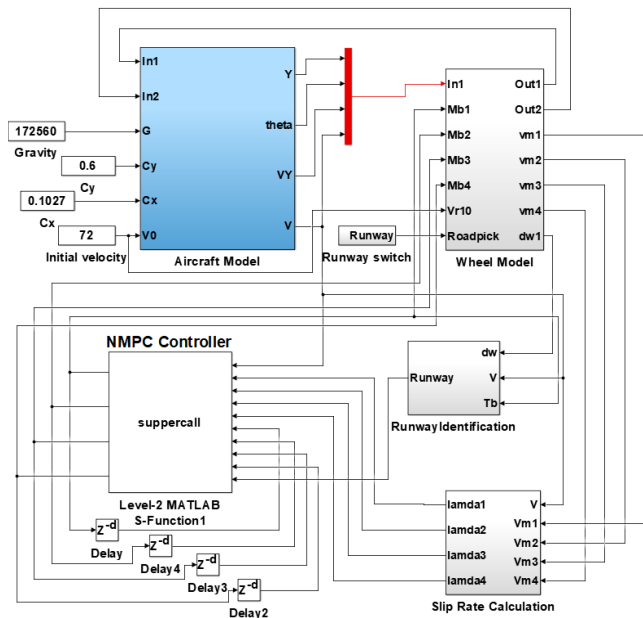


FIGURE 7. Aircraft full-vehicle brake control model in MATLAB/Simulink.

TABLE 1. Main parameters of aircraft brake system used in simulations.

Symbol	Parameter	Value
$m$	Aircraft mass	17256kg
$H$	Initial height of the aircraft c.g.	2.178m
$b$	Distance from c.g. to the front axle	6.727m
$a$	Distance from c.g. to the rear axle	1.076m
$r$	Rolling radius of the tire	0.4m
$J$	Rotational inertia of the rear wheel	1.885kgm <sup>2</sup>
$k_x$	Longitudinal air resistance coefficient	0.1027
$k_y$	Air lift coefficient	0.6
$v_0$	Initial value of aircraft speed	72m/s

the slip rate be closer to the stable region. The main aircraft parameters used in the simulation are listed in Table 1.

The control performances of the slip-NMPC, MSD-Pressure-Bias-Modulated (MSD-PBM), and MSD-NMPC algorithms were compared on a specific mixed runway. The slip-NMPC represents a slip-based NMPC controller that uses the slip rate as an NMPC control variable instead of a combination of the slip rate and deceleration rate. The PBM controller refers to a proportional-derivative controller with a multi-threshold integral module [26]. The MSD-PBM controller is based on a mixed control variable as follows:

$$y = y_{PD} + y_{PBM} = (K_P \cdot \Delta\varepsilon + K_D \cdot \Delta\dot{\varepsilon}) + y_{PBM}$$

$$y_{PBM} = \begin{cases} y'_{PBM} + \int (\Delta\varepsilon - \Delta\varepsilon_{T1}) dt & \Delta\varepsilon_{T1} \leq \Delta\varepsilon < \Delta\varepsilon_{T2} \\ y''_{PBM} + \int K_1 dt & \Delta\varepsilon \geq \Delta\varepsilon_{T2} \\ y'''_{PBM} - \iint K_2 dt dt & \Delta\varepsilon < \Delta\varepsilon_{T1} \end{cases}$$

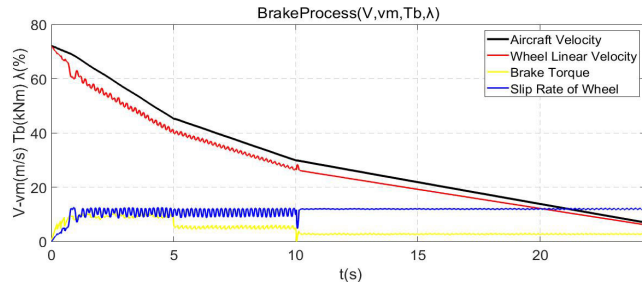


FIGURE 8. Braking process under the slip rate-based NMPC control on the mixed runway using ideal runway identification results.

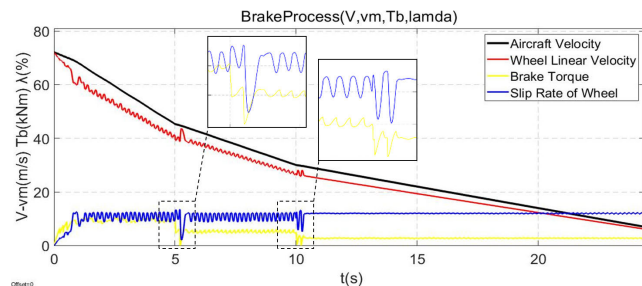


FIGURE 9. Braking process under the slip rate-based NMPC control on the mixed runway using the proposed runway identification method.

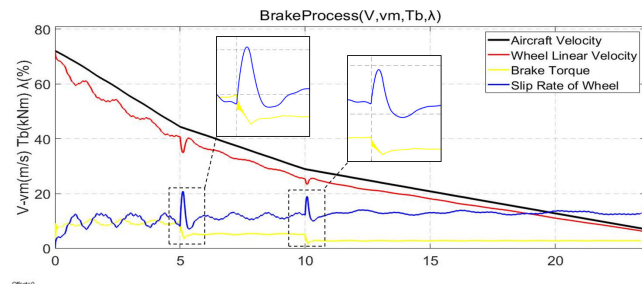


FIGURE 10. Braking process under the MSD-PBM control on the mixed runway using the proposed runway identification method.

$$\Delta\varepsilon = \varepsilon - \varepsilon_r = (\alpha\lambda + (1 - \alpha)\eta) - \varepsilon_r \quad (19)$$

where  $y$  denotes the MSD-PBM controller output,  $K_P$ ,  $K_D$  denote the coefficients of proportional-derivative controller,  $y_{PBM}$  denotes the output voltage of the PBM, and  $y'_{PBM}$ ,  $y''_{PBM}$ ,  $y'''_{PBM}$  denote the  $y_{PBM}$  values at the state turning points;  $\Delta\varepsilon$  is the difference between the system output  $\varepsilon$  and desire output  $\varepsilon_r$ , and  $\Delta\varepsilon_{T1}$  and  $\Delta\varepsilon_{T2}$  are the lower and upper threshold values of the PBM;  $K_1$  is the voltage rising speed, and  $K_2$  is the voltage reducing speed.

## B. SIMULATION RESULTS AND ANALYSIS

### 1) MIXED RUNWAY CONDITION

The mixed runway structure was as follows: dry runway in the interval of 0–5 s, wet runway in the interval of 5–10 s, and ice runway after 10 s; the runway models were as given in Section II. The velocity, output pressure, and slip rate of the dynamic braking process for different control schemes and controller parameters are shown in Figs. 8–12. The slip

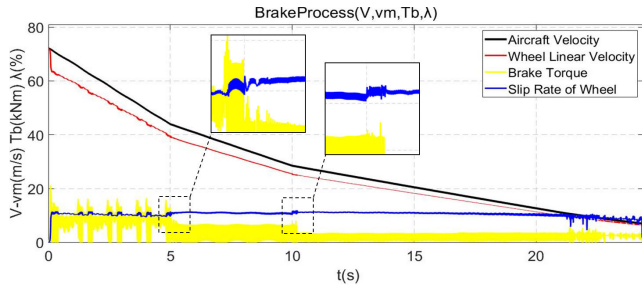


FIGURE 11. Braking process under the MSD-NMPC control on the mixed runway using the proposed runway identification method ( $P_1 = 2 \times 10^{-7}$ ).

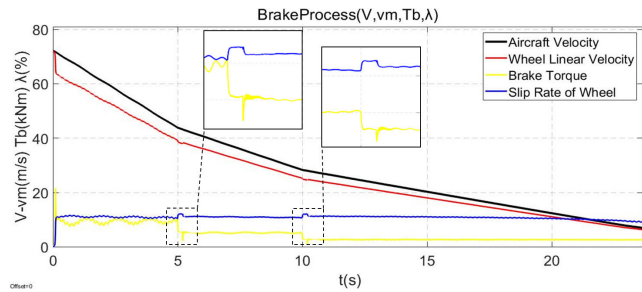


FIGURE 12. Braking process under the MSD-NMPC control on the mixed runway using the proposed runway identification method (tuned  $P_1 = 2 \times 10^{-6}$ ).

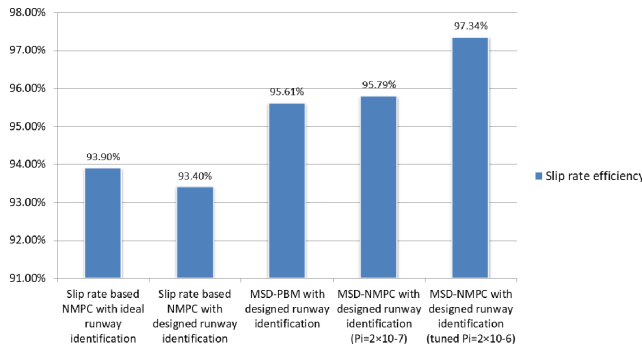


FIGURE 13. Slip rate efficiency of different control algorithms on the mixed runway.

rate efficiency under different braking conditions is shown in Fig. 13, and it was calculated by the method referred to as the Flight Test Guide for Certification of Transport Category Airplanes (AC25-7D) [27], which is as follows:

$$\begin{cases} WSR < OPS & eff = 1.5 \left( \frac{WSR}{OPS} \right) - 0.5 \left( \frac{WSR}{OPS} \right)^3 \\ WSR = OPS & eff = 1.0 \\ WSR > OPS & eff = 0.5 \left( 1 + \frac{(1 - WSR)}{(1 - OPS)} \right) \\ EFFICIENCY & = \frac{\int eff \cdot dS}{S} \end{cases} \quad (20)$$

where  $WSR$  represents the wheel slip rate,  $OPS$  is the optimal slip rate,  $eff$  is the instantaneous slip efficiency,  $S$  is the

stopping distance, and  $EFFICIENCY$  is the slip efficiency of the whole braking process.

The lag of runway status identification could lead to the delay in model switching of the NMPC, resulting in a short period of model mismatch. From the control effect results presented in Figs. 9, 11, and 12, the reduction in control performance was acceptable, while the system stability in a finite time was not affected.

The tracking target of the MSD-PBM control was adjusted using the proposed runway identification method. The results presented in Fig. 10 were obtained under the manually-tuned PBM controller parameters. As shown in Fig. 10, a deep slip occurred after the runway switch and automatically recovered after 0.2–0.4 s. This could hardly be prevented since the PBM control scheme based on fixed parameters could not handle the changes in system characteristics. The slip depth was reduced using the adaptive parameters tuning method; even so, the brake efficiency was up to 95.61%. In contrast, the MSD-NMPC controller had a much better control effect, as shown in Fig 12; the braking process was more stable, and the slip overstrike of the runway switch was much less due to the prediction model adjustment based on the runway identification.

The slip rate could be controlled within the optimal value using different NMPC control algorithms, as shown in Figs. 8, 9, 11, and 12. As shown in Figs. 9 and 11, the MSD-based NMPC controller had smaller slip rate fluctuation and tracking error than the slip-based NMPC, which ultimately improved the brake efficiency; also, the deep slip after the runway switch was successfully controlled under this condition.

In meanwhile, a better control effect was achieved by tuning the weighting matrix  $P$ . The brake torque output changed more smoothly at a larger  $P$ . The MSD-based NMPC control with a tuned weighting matrix  $P$  achieved the highest brake efficiency of 97.34% among all algorithms, as shown in Fig. 13. The weighting matrix obtained by tuning was sub-optimal, while the optimal problem of the weighting matrix was not discussed in this paper. Consequently, the proposed MSD-NMPC control method can adapt to different runway conditions. In addition, the braking efficiency of the proposed method on the mixed runway is significantly higher than those of the other control methods, and its slip rate overshoot is smaller when the tire-runway state is switched.

## 2) MIX RUNWAY WITH MEASUREMENT NOISE

In order to verify the sensitivity of MSD-NMPC algorithm to measurement noise, we introduce the wheel speed measurement noise and slip rate estimation error in dry runway condition as shown in Fig. 14, which are referred collectively as measurement noises. Zero mean band-limited white noises are superimposed in the slip rate signal and deceleration rate signal as estimation error and measurement noise. Due to poor aircraft vehicle estimation, the estimation error of slip rate has larger variance than deceleration rate while characterized by huge spikes at the same time.

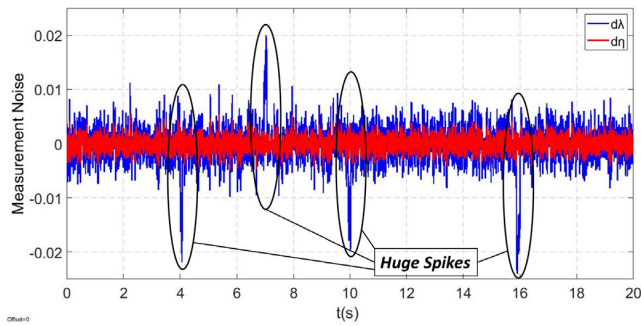


FIGURE 14. Measurement noises of the wheel deceleration and estimation error of wheel slip.

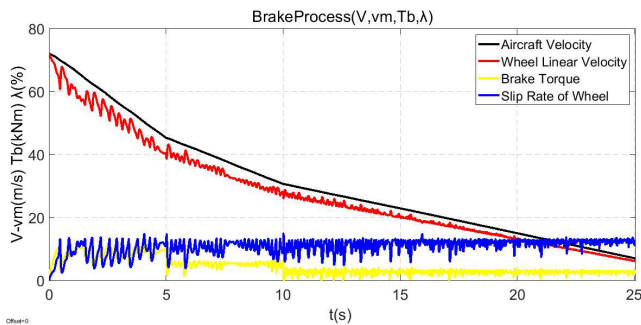


FIGURE 15. Brake process of slip-NMPC control on dry runway with measurement noises.

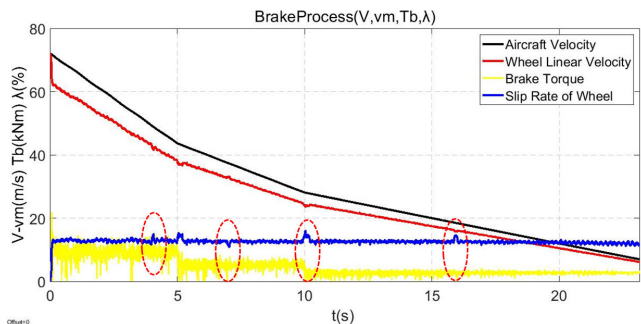


FIGURE 16. Brake process of MSD-NMPC control on dry runway with measurement noises.

The slip-NMPC and MSD-NMPC control methods with measurement noises in mixed runway condition are compared to demonstrate the advantages of the MSD control strategy. The braking performances of two methods are respectively shown in Fig. 15 and 16.

By comparing the previous simulation results with no measurement noises, it can be seen that the braking process is all affected by the measurement noises. Especially for the slip-NMPC method, with the slip rate fluctuating dramatically near the reference value and the tracking error increasing, the braking efficiency decreases in the condition of measurement noises, as compared in Fig. 17. However, we find that the MSD-NMPC method has a better insensitivity against the measurement noises than slip-NMPC, since the fluctuation of the slip rate affected by noise is relatively small, and even for

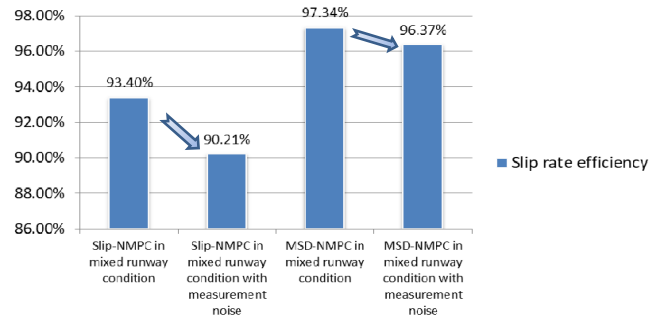


FIGURE 17. Slip rate efficiency changes of NMPC control algorithms on dry runway with measurement noises.

huge spikes the noise doesn't cause significant disturbance to the system, as shown in Fig. 16. So it has smaller braking efficiency decrease and significantly better braking performance.

### V. CONCLUSION

In this paper, an MSD-based NMPC aircraft anti-skid brake control method with runway identification is proposed to improve the braking performance while considering the braking torque limitations, wheel slip constraints, and performance metrics. A runway identification algorithm is used to adjust the parameters of the prediction model under the switching runway conditions. The proposed controller is verified by the tricycle-gear aircraft model built in MATLAB/Simulink. The simulation results show that the proposed MSD-based NMPC controller can accurately control the wheel longitudinal slip rate within the optimal value and effectively prevent the wheel from locking up during the braking process under switching-runway conditions. This study considers only the longitudinal aircraft dynamics and ignores the lateral characteristics, so the proposed controller cannot handle complex asymmetric cases, which will be addressed in our future work.

### REFERENCES

- [1] M. Martinez-Gardea, I. J. M. Guzman, S. Di Gennaro, and C. A. Lua, "Experimental comparison of linear and nonlinear controllers applied to an antilock braking system," in *Proc. IEEE Conf. Control Appl. (CCA)*, Juan Les Antibes, France, Oct. 2014, pp. 71–76, doi: 10.1109/CCA.2014.6981331.
- [2] H. Song, B. Fang, and P. Wang, "Research and applications of immune PID adaptive controller in anti-skid braking system for aircraft," in *Proc. Int. Conf. Inf. Eng. Comput. Sci.*, Wuhan, China, Dec. 2009, pp. 1–5, doi: 10.1109/ICIECS.2009.5363257.
- [3] Y. H. Han and M. A. Xiao-Ping, "Application of fuzzy PID controller in the electric brake system of aircraft," *Aeronaut. Comput. Technique*, vol. 37, no. 5, pp. 103–105, 2007.
- [4] M. Schinkel and K. Hunt, "Anti-lock braking control using a sliding mode like approach," in *Proc. Amer. Control Conf.*, Anchorage, AK, USA, 2002, pp. 2386–2391, doi: 10.1109/ACC.2002.1023999.
- [5] M.-B. Radac and R.-E. Precup, "Data-driven model-free slip control of anti-lock braking systems using reinforcement Q-learning," *Neurocomputing*, vol. 275, pp. 317–329, Jan. 2018.
- [6] K.-S. Park and J.-T. Lim, "Wheel slip control for ABS with time delay input using feedback linearization and adaptive sliding mode control," in *Proc. Int. Conf. Control, Autom. Syst.*, Seoul, South Korea, Oct. 2008, pp. 290–295, doi: 10.1109/ICCAS.2008.4694658.



- [7] M. Tanelli, A. Astolfi, and S. M. Savaresi, "Robust nonlinear output feedback control for brake by wire control systems," *Automatica*, vol. 44, no. 4, pp. 1078–1087, Apr. 2008.
- [8] C. Unsal and P. Kachroo, "Sliding mode measurement feedback control for antilock braking systems," *IEEE Trans. Control Syst. Technol.*, vol. 7, no. 2, pp. 271–281, Mar. 1999, doi: [10.1109/87.748153](https://doi.org/10.1109/87.748153).
- [9] Jin, Yin, and Chen, "Advanced estimation techniques for vehicle system dynamic state: A survey," *Sensors*, vol. 19, no. 19, p. 4289, Oct. 2019.
- [10] F. Gustafsson, "Slip-based tire-road friction estimation," *Automatica*, vol. 33, no. 6, pp. 1087–1099, Jun. 1997.
- [11] M. Tanelli and S. M. Savaresi, "Friction-curve peak detection by wheel-deceleration measurements," in *Proc. IEEE Intell. Transp. Syst. Conf.*, Toronto, ON, Canada, Sep. 2006, pp. 1592–1597, doi: [10.1109/ITSC.2006.1707451](https://doi.org/10.1109/ITSC.2006.1707451).
- [12] C. Canudas-De-Wit, M. L. Petersen, and A. Shiriaev, "A new nonlinear observer for tire/road distributed contact friction," in *Proc. 42nd IEEE Int. Conf. Decis. Control*, Maui, HI, USA, vol. 3, Dec. 2003, pp. 2246–2251, doi: [10.1109/CDC.2003.1272952](https://doi.org/10.1109/CDC.2003.1272952).
- [13] E. Ono, K. Asano, M. Sugai, S. Ito, M. Yamamoto, M. Sawada, and Y. Yasui, "Estimation of automotive tire force characteristics using wheel velocity," *Control Eng. Pract.*, vol. 11, no. 12, pp. 1361–1370, Dec. 2003.
- [14] L. Yuan, H. Zhao, H. Chen, and B. Ren, "Nonlinear MPC-based slip control for electric vehicles with vehicle safety constraints," *Mechatronics*, vol. 38, pp. 1–15, Sep. 2016.
- [15] B. Ren, H. Chen, H. Zhao, and L. Yuan, "MPC-based yaw stability control in in-wheel-motored EV via active front steering and motor torque distribution," *Mechatronics*, vol. 38, pp. 103–114, Sep. 2016.
- [16] Y. Ma, J. Zhao, H. Zhao, C. Lu, and H. Chen, "MPC-based slip ratio control for electric vehicle considering road roughness," *IEEE Access*, vol. 7, pp. 52405–52413, 2019, doi: [10.1109/ACCESS.2019.2910891](https://doi.org/10.1109/ACCESS.2019.2910891).
- [17] P. Wang, Z. Liu, Q. Liu, and H. Chen, "An MPC-based manoeuvre stability controller for full drive-by-wire vehicles," *Control Theory Technol.*, vol. 17, no. 4, pp. 357–366, Nov. 2019.
- [18] P. Mhaskar, N. H. El-Farra, and P. D. Christofides, "Stabilization of nonlinear systems with state and control constraints using Lyapunov-based predictive control," *Syst. Control Lett.*, vol. 55, no. 8, pp. 650–659, Aug. 2006.
- [19] W. Pasillas-Lépine and A. Loria, "A new mixed wheel slip and acceleration control based on a cascaded design," *IFAC Proc.*, vol. vol., 43, no. 14, pp. 879–884, 2010.
- [20] M. Q. Chen, W. S. Liu, Y. Z. Ma, J. Wang, F. R. Xu, and Y. J. Wang, "Mixed slip-deceleration PID control of aircraft wheel braking system," *IFAC-Papers Line*, vol. 51, no. 4, pp. 160–165, 2018.
- [21] S. M. Savaresi, M. Tanelli, and C. Cantoni, "Mixed slip-deceleration control in automotive braking systems," *J. Dyn. Syst., Meas., Control*, vol. 129, no. 1, pp. 20–31, Jul. 2006.
- [22] P. Falcone, F. Borrelli, H. E. Tseng, J. Asgari, and D. Hrovat, "Linear time-varying model predictive control and its application to active steering systems: Stability analysis and experimental validation," *Int. J. Robust Nonlinear Control*, vol. 18, no. 8, pp. 862–875, 2008.
- [23] P. Dworak, J. K. Goyal, S. Aggarwal, and S. Ghosh, "Effective use of MPC for dynamic decoupling of MIMO systems," *Elektronika Elektrotehnika*, vol. 25, no. 2, pp. 3–8, Apr. 2019.
- [24] H. B. Pacejka and E. Bakker, "The magic formula tyre model," *Vehicle Syst. Dyn.*, vol. 21, no. 1, pp. 1–18, Jan. 1992.
- [25] P. E. Gill, W. Murray, and M. A. Saunders, "SNOPT: An SQP algorithm for large-scale constrained optimization," *SIAM Rev.*, vol. 47, no. 1, pp. 99–131, Jan. 2005.
- [26] S. M. Stubbs and J. A. Tanner, "Behavior of aircraft antiskid braking systems on dry and wet runway surfaces: A velocity-rate-controlled, pressure-bias-modulated system," NASA Langley Research Center, Hampton, VA, USA, Tech. Rep. NASA TN D-8332, Dec. 1976.
- [27] *Flight Test Guide for Certification of Transport Category Airplanes*, document AC25-7D, 2018.



**MENGQIAO CHEN** received the B.S. degree in automation from the School of Astronautics, Harbin Institute of Technology, Harbin, China, in 2011, and the M.S. degree in control engineering from Central South University, Changsha, China, in 2014, where he is currently pursuing the Ph.D. degree in control theory and control engineering with the School of Automation. His research interests include brake control systems and anti-skid brake control of aircraft.



**FENGRUI XU** received the B.S. degree in automation from the College of Information Science and Engineering, Harbin Institute of Technology, Weihai, China, in 2012, and the M.S. degree in control engineering from the Central South University, Changsha, China, in 2016, where he is currently pursuing the Ph.D. degree in control theory and control engineering with the School of Automation. His current research interests include nonlinear bifurcation and singularity phenomenon of anti-skid braking systems.



**XUELIN LIANG** received the B.S. degree in automation from Central South University, in 2013, and the M.S. degree in control theory and control engineering, in 2015. He is currently pursuing the Ph.D. degree with the School of Automation, Central South University. His research interests include stochastic control, artificial intelligence, and aircraft electric brake control systems.



**WENSHENG LIU** received the B.S. degree in nonferrous metallurgy, and the M.S. and Ph.D. degrees in materials science from Central South University, Changsha, China, in 1990, 1997, and 2008, respectively.

He is currently a Cheung Kong Scholar specially-appointed Professor and New Century Excellent Talents of the Ministry of Education and a Ph.D. Tutor, and the Director of the Advanced Research Center, Central South University. His main academic positions are the Director of the National Key Laboratory of Science and Technology on High-strength Structural Materials and the Deputy Director of the National Engineering Research Center of Powder Metallurgy. His research interests include powder metallurgy materials, electronic materials, lightweight structural materials, and aviation braking systems.

• • •